

Original Article

Quantitative proteomics analysis of mitochondrial proteins in lung adenocarcinomas and normal lung tissue using iTRAQ and tandem mass spectrometry

Wei Li¹, Xuede Zhang², Wei Wang¹, Ruiying Sun¹, Boxuan Liu¹, Yuefeng Ma³, Wei Zhang³, Li Ma⁴, Yaofeng Jin⁴, Shuanying Yang¹

¹Department of Respiratory Medicine, Second Affiliated Hospital of Xi'an Jiaotong University, Xi'an 710004, Shaanxi Province, P. R. China; ²Department of Oncology, Shandong Provincial Qianfoshan Hospital, Shandong University, Jinan 250014, Shandong Province, P. R. China; ³Department of Thoracic Surgery, Second Affiliated Hospital of Xi'an Jiaotong University, Xi'an 710004, Shaanxi Province, P. R. China; ⁴Department of Pathology, Second Affiliated Hospital of Xi'an Jiaotong University, Xi'an 710004, Shaanxi Province, P. R. China

Received May 17, 2017; Accepted August 14, 2017; Epub September 15, 2017; Published September 30, 2017

Abstract: Lung adenocarcinoma is the most common type of lung cancer. Unfortunately, lung adenocarcinoma has a poor prognosis and the pathogenesis remains unclear. Mitochondria are important mediators of tumorigenesis. However, the proteomics profile of lung adenocarcinoma mitochondrial proteins has not been elucidated. In this study, we investigated differences in the mitochondrial protein profiles between lung adenocarcinomas and normal tissue. Laser capture microdissection (LCM) was used to isolate the target cells from lung adenocarcinomas and normal tissue. The differential expression of mitochondrial proteins was determined using isobaric tags for relative and absolute quantitation (iTRAQ) combined with two-dimensional liquid chromatography-tandem mass spectrometry (2D-LC-MS/MS). Bioinformatics analysis was performed using Gene Ontology and KEGG databases. As a result, 510 differentially expressed proteins were identified, 315 of which were upregulated and 195 that were downregulated. Of these proteins, 35.5% were mitochondrial or mitochondrial-related and were involved in binding, catalysis, molecular transduction, transport, and molecular structure. Based on the differentially expressed proteins, 63 pathways were significantly enriched through KEGG. The overexpression and cellular distribution of the mitochondrial protein C1QBP in the lung cancer samples was confirmed and verified by Western blotting. The relationship between C1QBP expression and clinicopathological features in lung cancer patients was likewise evaluated using immunohistochemistry, which revealed that the upregulation of C1QBP was associated with lymph node metastasis, pathological grade and clinical stage of TNM. The results indicate that the iTRAQ 2D-LC-MS/MS technique is a potential method for comparing mitochondrial protein profiles between tumor and normal tissue and could aid in identifying novel biomarkers and the mechanisms underlying carcinogenesis.

Keywords: Lung adenocarcinoma, iTRAQ, mitochondrial protein, proteomic profile

Introduction

Lung cancer is the leading cause of cancer deaths worldwide [1], especially in China [2]. Further, the most common type of lung cancer is lung adenocarcinoma, which is associated with morbidity and mortality rates that continue to rise [3]. The average 5-year survival of lung adenocarcinoma cancer patients is only approximately 15% [4]. As well, although many treatments are available, its prognosis remains poor. Thus, discovering a novel early prognostic

marker of aggressive lung adenocarcinoma is critical.

Mitochondria are essential membrane-bound, subcellular organelles involved in cell survival in eukaryotes. Mitochondria are not only key organelles for ATP production, but also are also the major source of reactive oxygen species (ROS), and participate in multiple signaling cascades, including apoptosis. In stress sensing, mitochondrial protein expression is altered to allow for cellular adaptation to the environment.

Mitochondrial proteomic between lung adenocarcinomas and normal lung tissue

The oncogene *c-Myc* also affects mitochondrial dynamics by altering the expression of multiple fission and fusion proteins [5]. As well, the balance of pro- and anti-apoptotic proteins could affect the susceptibility of cancer cells to apoptotic stimuli and might predict the response of a tumor to chemotherapy [6]. The p53 tumor proteins also function in the regulation of cellular metabolism via the transcriptional activation of metabolic genes [7]. Thus, alterations in the expression of mitochondrial proteins could reflect the initiation, growth, survival, and metastasis of disease, including lung cancer [8, 9].

Quantitative proteomics provides a new opportunity to identify differentially expressed proteins in normal and tumor tissues. As well, comparative proteomics has the potential to reveal underlying molecular mechanisms of disease. However, the heterogeneity of the soft tumor tissues is a primary obstacle in proteomics analyses. Laser capture microdissection (LCM) is one of the best technologies for purifying target cells from heterogeneous tissues. Likewise, isobaric tags for relative and absolute quantification (iTRAQ) is a relatively new technique in quantitative proteomics that can be used to identify and quantify the protein expression levels and to detect small changes in protein expression in different tissues.

In this study, LCM was used to purify the target cells from lung cancer tissues and matched normal tissues, and iTRAQ followed by two-dimensional liquid chromatography-tandem mass spectrometry (2D-LC-MS/MS) using mass spectrometer was performed to separate and identify the differentially expressed mitochondrial proteins in lung adenocarcinomas and normal tissue. The C1QBP protein was overexpressed in lung adenocarcinomas compared with normal lung tissue, which was confirmed in clinical samples by Western blotting and immunohistochemistry.

Materials and methods

Human tissue samples

For LCM, lung adenocarcinoma and matched adjacent normal lung tissue samples were obtained from 10 patients who underwent sur-

gery at the Second Affiliated Hospital of the Xi'an Jiaotong University Medical School (age, 40-69 years; mean, 55.1 years; SD, 8.6). The adjacent normal tissues obtained were at least 5 cm away from the primary tumor. All samples were immediately embedded in Tissue-Tek® Optimal Cutting Temperature (O.C.T) medium (Sakura® Finetek, Fisher Scientific, Pittsburgh, PA, USA) and immediately stored at -80°C in liquid nitrogen until analyzed. The mitochondrial proteins from the lung cancer and matched normal lung tissues were used for comparative proteomics analysis and Western blotting.

For the immunohistochemistry analysis, 46 formalin-fixed, paraffin-embedded lung cancer specimens (26 lung adenocarcinoma and 20 lung squamous cell carcinoma) and 24 normal lung tissues acquired during surgical resections were obtained from the Second Affiliated Hospital, Xi'an Jiaotong University and Shaanxi Cancer Hospital for this retrospective study.

All of the procedures described here in were approved by the local ethics committee, and all patients who participated in the study provided informed consent.

Laser capture microdissection

The PixCell was used to capture the cells of interest from the frozen lung adenocarcinoma and matched adjacent normal lung tissue sections using a Laser Capture Microdissection Microscope (ARCTURUS Inc., USA) as described by Bonner et al [10]. The LCM conditions included a laser beam diameter of 7.5 μ m, a duration of 15.5 ms, and an energy of 80 mW. To diminish the effects of the biological variation across the samples on the results of the proteomics analysis, equal amounts of protein obtained from the cells following LCM of samples from 10 different individuals were pooled to generate one common sample for iTRAQ labeling.

Purification of cell mitochondrial proteins

The tissues were minced on ice and homogenized using a Dounce homogenizer and pre-chilled homogenization buffer (250 mM sucrose, 10 mM Tris-HCl, pH 7.4). The filtered homogenate was then centrifuged at 1,500 \times g

Mitochondrial proteomic between lung adenocarcinomas and normal lung tissue

for 10 min and the supernatant was removed and centrifuged at 4°C at 10,000 × g for 30 minutes, which yielded the mitochondrial proteins in the sediment. The supernatant was collected as a control and used to assess the purity of the extracted membrane proteins by Western blotting. The concentration of the mitochondrial proteins was assayed by the Bradford method. The purity of the isolated proteins was validated by Western blotting using a mitochondrial marker, the plasma membrane marker cytochrome c oxidase, and Na⁺/K⁺-ATPase.

Strong cation exchange chromatography

The iTRAQ labeled peptides were mixed and fractionated by strong cation exchange (SCX) chromatography using an HPLC system (Agilent) and a Phenomenex Luna[®] 5 μm SCX 100Å Column (250 × 4.60 mm; Phenomenex). Buffer A (25% ACN, 10 mM KH₂PO₄, pH 3.0) and buffer B (25% ACN, 10 mM KH₂PO₄, 2 M KCl, pH 3.0) were used as the mobile phases for gradient separation at a flow rate of 1 ml/min. The elution gradient was as follows: 25 min, 0% B; 1 min, 0-5% B; 20 min, 5-30% B; 5 min, 30-50% B; 5 min, 50% B; 5 min, 50-100% B; and 10 min, 100% B. The fractions were collected at one-minute intervals, lyophilized in a vacuum concentrator, and subsequently desalted using a Strata[®]-X C18 column.

NanoLC-MS/MS analysis

According to the workflow, the peptides were analyzed on a QExactive Mass Spectrometer (Thermo Fisher Scientific, MA, USA) equipped with an UltiMate™ 3000 nanoHPLC system (Dionex). The desalted fractions were loaded onto a homemade analytical column [Venusil XBP, C18 (L), 75 mm × 150 mm, 5 μm, 150Å, Agela Technologies] and separated using a mobile phase containing buffer A (H₂O + 0.1% formic acid) and buffer B (acetonitrile + 0.1% formic acid) at 400 nl/min. The gradient separation was performed as follows: 10 min, 5% B; 30 min, 5-30% B; 5 min, 30-60% B; 3 min, 60-80% B; 7 min, 80% B; 3 min, 80-% B; and 7 min, 5% B. A full mass scan was performed in data-dependent mode using the QExactive™ mass spectrometer. The scan range was set from 350-2000 *m/z* at 70,000 resolution (*m/z*

200). The automatic gain control (AGC) target was set to 3.00 × 10⁶ with a maximum ion injection time (IT) of 50 ms. In the MS scan, the 20 most abundant ions with charge states of +2 to +7 were selected for MS2 fragmentation via higher-energy collisional dissociation (HCD) at an isolation width of 2.0 *m/z* and a normalized collision energy of 28%. Tandem mass spectra were acquired in profile mode at a resolving power of 17,500 at *m/z* 200 with an AGC target of 1 × 10⁵ and a maximum IT of 100 ms. For each scan, the dynamic exclusion was set to 15 s.

Identification and quantitation of mitochondria proteins

Identification of labeled tryptic peptides was performed using Proteome Discoverer (version 1.3, Thermo Scientific). Raw files were searched against databases consisting of the appropriate protein sequences (Uniprot) and Mascot Version 2.3.0. Peptides were produced by digestion with trypsin with a maximum of one missed cleavages and were matched using precursor and fragment mass tolerances of 15 ppm and 0.02 Da, respectively. Carbamidomethylation of cysteine was set as a fixed modification while oxidation of methionine, Gln→Pyro-Glu (N-term Q), iTRAQ 8 plex labeling at N-terminal, K, and Y were used as variable modifications. At least one unique peptide were required in protein quantification. less than 1% FDR was acceptable for both the peptide and protein level.

Bioinformatics analysis

The theoretical isoelectric point (pI) and molecular weight (MW) of the identified proteins were obtained from the Swiss-Prot protein sequence data bank. Gene Ontology (GO) analysis was performed to determine the main function of the differentially expressed genes according to GO, which is the key NCBI functional classification [11]. As well, pathway analysis was used to determine the significant pathways of the differentially expressed genes using the pathway annotations of microarray genes downloaded from KEGG (<http://www.genome.jp/keGG/>). A Fisher's exact test was used to determine the significant enrichment pathways and the resulting *p*-values were adjusted using the Benjamini

Mitochondrial proteomic between lung adenocarcinomas and normal lung tissue

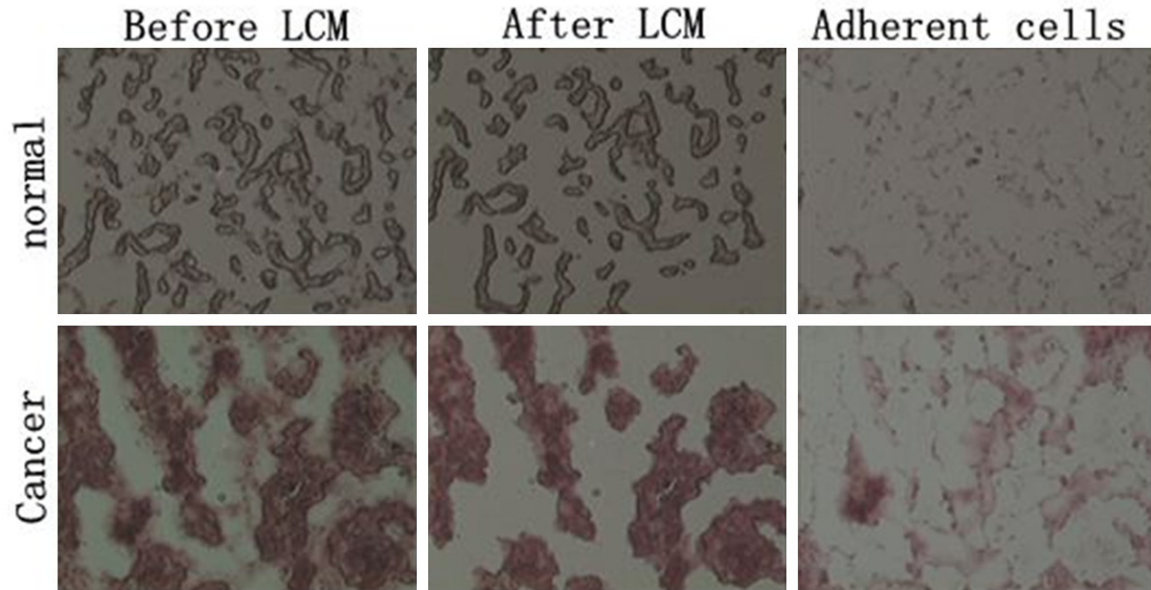


Figure 1. Laser capture microdissection of hematoxylin and eosin stained lung adenocarcinoma and paired normal lung tissue slides.

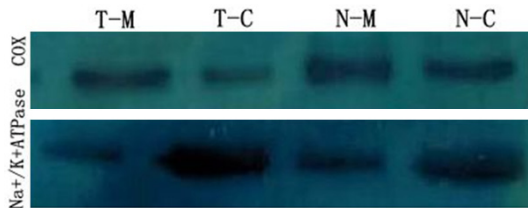


Figure 2. Western blot of purified mitochondrial fractions with cytochrome c oxidase (COX). Note: $\text{Na}^+/\text{K}^+\text{ATPase}$ is a mitochondrial protein marker and COX is a membrane protein marker; T-M represents the mitochondrial proteins in lung cancer tissues; T-C represents the lung cancer tissue cytosolic solutions; N-M represents the normal lung tissue mitochondrial proteins; N-C represents the normal lung tissue cytosolic solutions.

and Hochberg's false discovery rate (BH FDR) algorithm. Pathway categories with an FDR < 0.05 were reported.

Western blotting analysis

Western blotting analysis was performed for 10 pairs of fresh lung adenocarcinomas and normal lung tissue. The proteins (60 μg) were separated by SDS-PAGE and transferred to membranes. The membranes were blocked with 5% nonfat dry milk in TBST buffer for 2 h at room temperature, incubated with anti-C1QBP anti-

body (1:2000) overnight at 4°C, washed in TBST, and incubated again with horseradish peroxidase-conjugated secondary antibody (1:10000) for 2 h at room temperature. The immunoreactive protein bands were visualized by enhanced chemiluminescence and evaluated by densitometry using Image J software. β -actin was used as a loading control.

Immunohistochemistry and staining evaluation

C1QBP expression levels were determined using the standard streptavidin-horseradish peroxidase (SP) immunohistochemistry (IHC) technique. Paraffin embedded specimen sections (4 μm) were dewaxed, rehydrated in a series of ethanol solutions, and treated with an antigen retrieval solution in a microwave. Endogenous peroxidase activity was blocked using 3% H_2O_2 for 10 min. Non-specific staining was blocked for 15 min using normal goat serum. The sections were then incubated with anti-C1QBP antibody (1:200) overnight at 4°C. IHC was performed using the SP9001 Rabbit kit (ZhongshanJinqiao Biotech Company, Beijing, China) according to manufacturer's instructions. The immunoreaction was visualized using 3,3'-diaminobenzidine (DAB) staining. The sections were counterstained with hematoxylin and eosin, dehydrated, and then

Mitochondrial proteomic between lung adenocarcinomas and normal lung tissue

Table 1. Top 60 differentially expressed mitochondrial or mitochondria-related proteins in lung adenocarcinoma compared to normal lung tissue

Accession number	Description	Score	Coverage	Unique Peptides	PSMs	C/N
P01914	HLA class II histocompatibility antigen,	201.88	21.80%	2	23	0.158
Q14247	Src substrate cortactin	63.62	4.73%	2	4	0.212
Q8NFJ5	Retinoic acid-induced protein 3	68.93	3.64%	1	7	0.221
P01911	HLA class II histocompatibility antigen, DRB1-15 beta chain	335.97	42.48%	2	43	0.235
P16671	Platelet glycoprotein 4	279.22	15.89%	6	36	0.245
P55087	Aquaporin-4	95.97	6.19%	2	13	0.248
Q15109	Advanced glycosylation end product-specific receptor	216.94	17.82%	5	23	0.249
Q03135	Caveolin-1	361.65	65.17%	11	100	0.255
P51636	Caveolin-2	149.97	37.04%	4	16	0.275
P29972	Aquaporin-1	110.82	19.70%	2	15	0.286
Q9NX76	CKLF-like MARVEL transmembrane domain-containing protein 6	42.6	5.46%	1	3	0.295
P30486	HLA class I histocompatibility antigen, B-48 alpha chain	519.88	40.06%	1	78	0.298
O95810	Serum deprivation-response protein	171.99	20.24%	7	23	0.302
Q9BW04	Specifically androgen-regulated gene protein	24.14	2.50%	1	1	0.303
Q6NZI2	Polymerase I and transcript release factor	369.53	20.77%	7	66	0.305
P04439	HLA class I histocompatibility antigen, A-3 alpha chain	559.86	37.53%	1	117	0.307
P53680	AP-2 complex subunit sigma	44.42	11.27%	2	2	0.31
P62070	Ras-related protein R-Ras2	149.16	19.12%	1	22	0.312
Q9UGT4	Sushi domain-containing protein 2	469.98	16.42%	8	47	0.315
P57087	Junctional adhesion molecule B	50.3	9.73%	2	2	0.323
Q16853	Membrane primary amine oxidase	829.29	27.79%	18	258	0.325
P13928	Annexin A8 OS = Homo sapiens	184.7	16.21%	5	7	0.332
P11686	Pulmonary surfactant-associated protein C	103.09	14.72%	2	13	0.333
Q9NZN4	EH domain-containing protein 2	913.71	47.88%	22	125	0.335
Q10589	Bone marrow stromal antigen 2	73.37	10.00%	2	9	0.336
P10301	Ras-related protein R-Ras	281.04	38.53%	6	42	0.34
O00168	Phospholemman	27.34	13.04%	1	3	0.341
Q53TN4	Cytochrome b reductase 1	71.98	7.69%	2	5	0.342
Q9NRN5	Olfactomedin-like protein 3	75.77	6.16%	2	2	0.348
O94911	ATP-binding cassette sub-family A member 8	180	5.76%	6	8	0.352
P02747	Complement C1q subcomponent subunit C	114.71	16.33%	3	5	2.004
Q9HCY8	Protein S100-A14	184.4	61.54%	5	21	2.011
Q9BYC5	Alpha-(1,6)-fucosyltransferase	55.04	3.65%	2	3	2.018
P01876	Ig alpha-1 chain C region	653.58	56.09%	5	167	2.034
P84090	Enhancer of rudimentary homolog	74.31	32.69%	3	6	2.045
O43196	MutS protein homolog 5	28	0.84%	1	2	2.048
Q9HD45	Transmembrane 9 superfamily member 3	70.79	4.92%	3	10	2.057
P06454	Prothymosin alpha	89.12	12.61%	2	12	2.097
Q8N4H5	Mitochondrial import receptor subunit TOM5 homolog	33	13.73%	1	2	2.101
Q04695	Keratin, type I cytoskeletal 17	453.76	29.17%	6	42	2.121
P54886	Delta-1-pyrroline-5-carboxylate synthetase	343.75	16.35%	10	18	2.143
Q9GZT3	SRA stem-loop-interacting RNA-binding protein,	50.45	17.43%	2	2	2.144
P61604	10 kDa heat shock protein, mitochondrial	306.88	74.51%	8	64	2.147
Q9HAV4	Exportin-5	31.61	0.83%	1	1	2.155
Q04828	Aldo-ketoreductase family 1 member C1	295.12	29.41%	9	14	2.173
O60218	Aldo-ketoreductase family 1 member B10	237.75	21.84%	6	9	2.199
P10915	Hyaluronan and proteoglycan link protein 1	91.13	10.45%	3	4	2.205
P43490	Nicotinamidephosphoribosyltransferase	634.66	38.49%	15	59	2.231

Mitochondrial proteomic between lung adenocarcinomas and normal lung tissue

A8MW06	Thymosin beta-4-like protein 3	65.48	29.55%	3	13	2.233
P06889	Ig lambda chain V-IV region MOL	47.74	31.13%	2	2	2.49
P25815	Protein S100-P	103.01	24.21%	2	18	2.556
P02458	Collagen alpha-1(II) chain	129.15	3.30%	4	11	2.648
P49406	39S ribosomal protein L19,	36	3.77%	1	1	2.786
P21941	Cartilage matrix protein	187.68	8.67%	4	11	3.02
O95994	Anterior gradient protein 2 homolog	356.89	50.86%	8	120	3.028
P01605	Ig kappa chain V-I region Lay	60.5	25.00%	1	3	3.434
Q9H8P0	3-oxo-5-alpha-steroid 4-dehydrogenase 3	47.92	2.20%	1	2	3.448
Q8IWY8	Zinc finger and SCAN domain-containing protein 29	14.43	0.70%	1	2	3.593
P52926	High mobility group protein HMGI-C	30.05	17.43%	1	1	4.038
P04438	Ig heavy chain V-II region SESS	23.12	4.76%	1	2	4.083

Score: the sum of the scores of the individual peptides; Coverage: default the percentage of the protein sequence covered by identified peptides; Unique Peptides: the number of peptide sequences unique to a protein group; PSMs: The total number of identified peptide sequences (peptide spectrum matches) for the protein, including those redundantly identified; C: cancer; N: normal.

mounted with coverslips. The primary antibody was replaced with PBS as the negative control. All of the sections were examined microscopically and blindly evaluated by two independent pathologists according to a scoring method previously described by Yu [12]. At least five high-power fields were selected randomly, with >200 cells counted per field. The immunohistochemical score (IHS) was used to evaluate C1QBP based on the German immunoreactive score. The IHS was calculated by combining the staining intensity score with the quantity score (percentage of positive stained cells). Staining intensity was classified according to the following criteria: 0, no staining; 1, weak staining = light yellow; 2, moderate staining = yellow brown; and 3, strong staining = brown. The proportion of positive cells was scored as follows: 0 (no positive tumor cells), 1 (less than 10% of cells stained), 2 (10-50% of cells stained), and 3 (more than 50% of cells stained). The IHS was calculated by combining the staining intensity score with the quantity score (percentage of positive stained cells). Using this method, the expression of C1QBP in lung cancer tissues was evaluated by determining the staining index (scores 0-9). The combined staining score (staining intensity times staining area) was then graded as 0, negative expression; 1-4, low expression; and >4, high expression.

All observations and assessments were performed by two independent observers who were blinded to all clinical data. In all cases, there was less than 5% inter-observer variation in results. Cases with discrepancies were re-

viewed simultaneously by the original two pathologists and a senior pathologist until a consensus was reached.

Statistical analysis

Statistical analyses were performed using SPSS (Version 16.0; Chicago, IL, USA). The relationship between C1QBP expression levels and clinicopathological parameters was analyzed using the Mann-Whitney U or Kruskal-Wallis test. The C1QBP protein expression levels in lung cancer versus normal tissue were also analyzed using the Mann-Whitney U test. In all tests, two-sided *p*-values < 0.05 were considered statistically significant.

Results

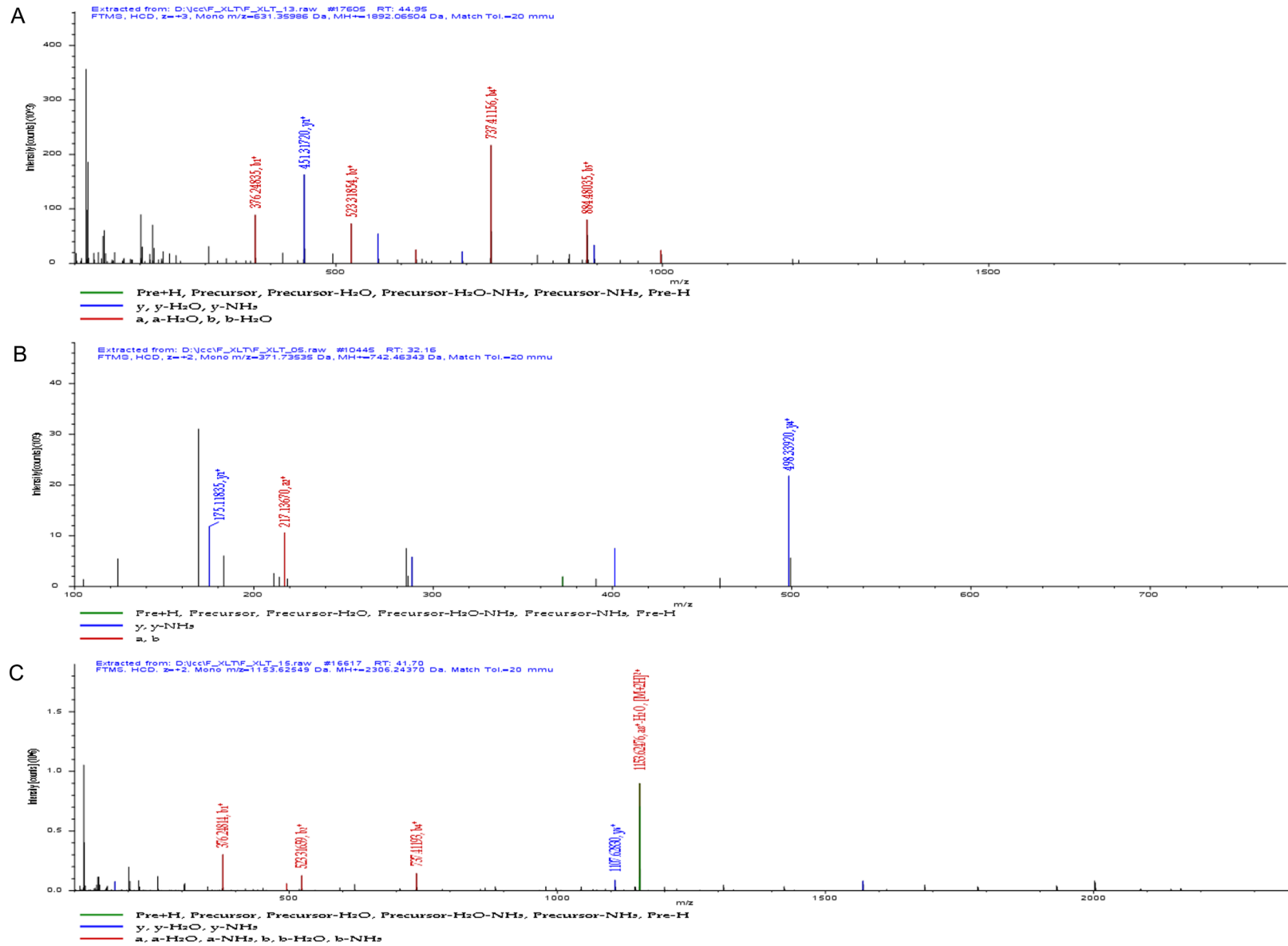
LCM

LCM was performed on lung cancer and surrounding normal tissue specimens to isolate tumor cells from non-tumor cells. Cryostat sections (8- μ m thickness) were stained with hematoxylin and eosin (H&E) prior to LCM. The cells of interest were collected on an LCM cap, whereas the interstitial tissues remained within the section after LCM (**Figure 1**). Each type of cell population on the LCM cap was estimated to be over 95% homogeneous as determined by microscopic visualization.

Validation of mitochondrial protein purification

Western blotting analysis was used to determine the purity of the extracted mitochondrial proteins. An analysis of the signal strength

Mitochondrial proteomic between lung adenocarcinomas and normal lung tissue



Mitochondrial proteomic between lung adenocarcinomas and normal lung tissue

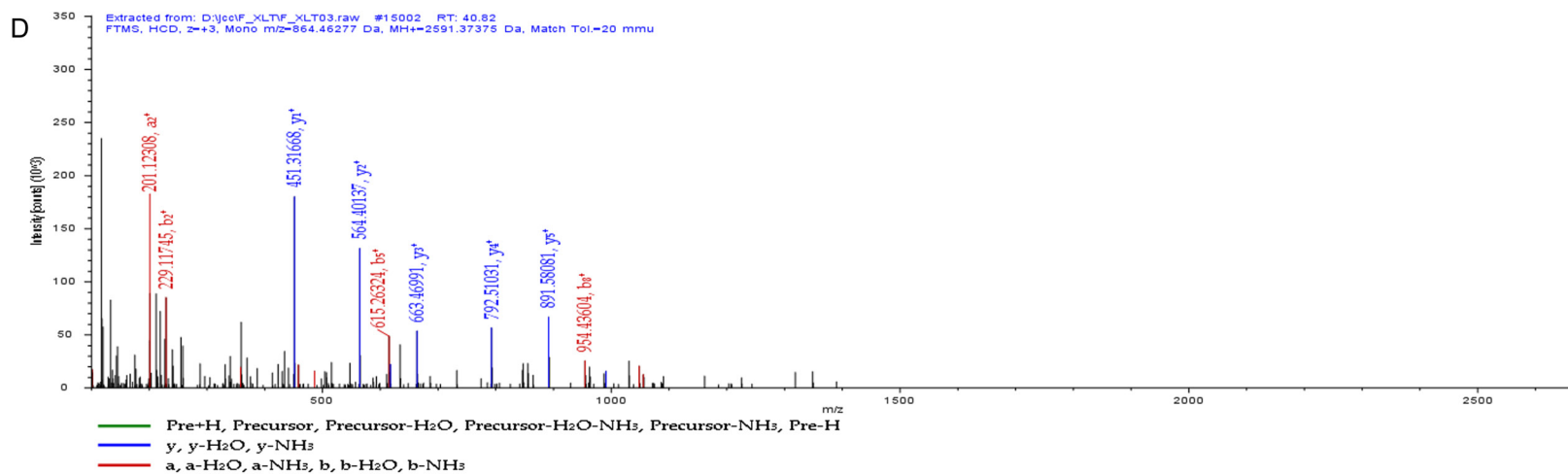


Figure 3. MS/MS spectra of four identified peptides: (A) the MS/MS spectra of aFVDFLSDEIk, with m/z of 946.53412 Da ($z = +2$), MH+: 1892.06096 Da. (B) The MS spectra of sequence MLPLLR with m/z of 371.73535 Da ($z = +2$), MH+: 742.46343 Da; (C) The MS spectra of sequence aFVDFLSDEIkEER with m/z of 1153.62549 Da ($z = +2$), MH+: 2951.60300 Da; (D) The MS spectra of sequence VEEQEPeLTSTPNFVVEIik with m/z of 864.46277 Da ($z = +3$), MH+: 2591.37375 Da.

Mitochondrial proteomic between lung adenocarcinomas and normal lung tissue

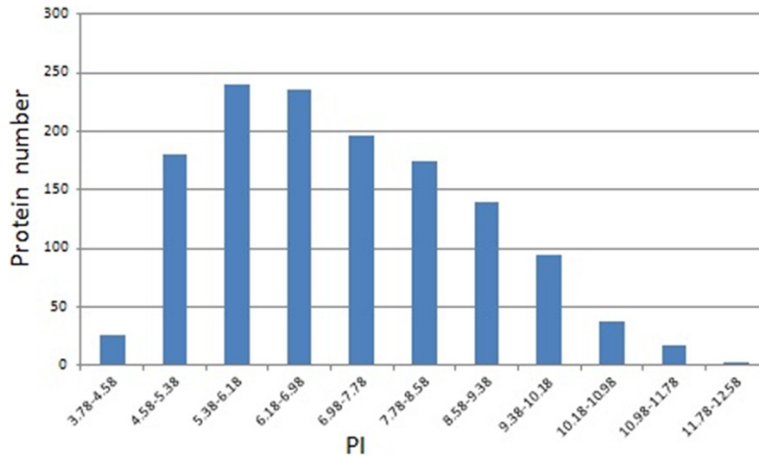


Figure 4. The molecular weight (MV) distribution of the identified proteins.

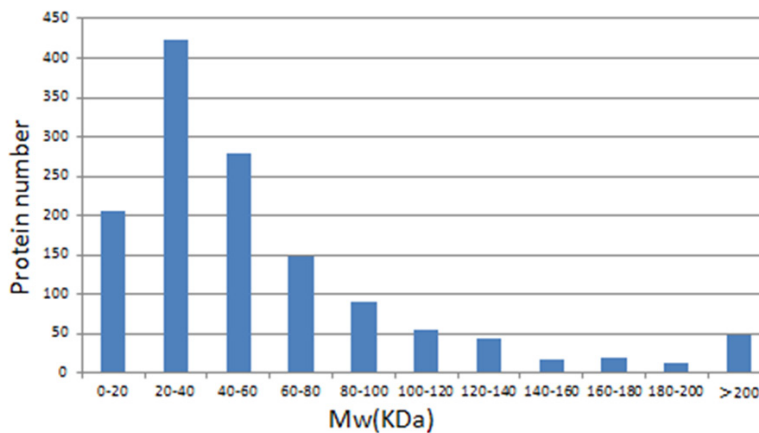


Figure 5. The isoelectric point (PI) distribution of the identified proteins.

using ImageJ software revealed that the plasma mitochondrial marker (cytochrome c oxidase) level was 5.7-fold and 5.6-fold higher in the mitochondrial protein solution compared with the cytoplasmic protein solution for lung adenocarcinomas and normal lung tissue, respectively. In contrast, the membrane marker (Na^+/K^+ -ATPase) levels were 3.1-fold and 3.3-fold lower in the mitochondrial protein solution compared with the cytoplasmic proteins for lung cancer and normal lung tissues, respectively (**Figure 2**). These results indicated that the mitochondrial proteins were successfully purified with lung cells by LCM.

Identification of differentially expressed proteins

In this study, we used iTRAQ labeling and 2D-LC-MS/MS to compare protein expression in pooled lung adenocarcinoma and matched

normal lung tissue samples. A total of 1343 different proteins were identified in the tumor and normal tissue samples based on at least one unique peptide assignment at $\geq 95\%$ confidence. Among the 1343 proteins, 510 proteins were considered differentially expressed between the lung adenocarcinoma and normal lung tissue according to ratios of fold-change (≥ 1.5 or ≤ 0.66). In addition, 315 proteins were upregulated and 195 were downregulated (**Table 1**). Referring to the literature, I found that many of these proteins are closely related to tumors. We further found that C1QBP is a mitochondrial protein that is closely related to tumor, but it is rarely reported in lung cancer. So we chose C1QBP for further study. Notably, C1QBP was significantly upregulated in lung adenocarcinomas (2.04-fold) compared with normal lung tissues. The MS/MS spectra of the four peptides assigned to C1QBP are shown in **Figure 3**.

Bioinformatics analysis of differentially expressed proteins

The MW of the differentially expressed proteins identified ranged from 5.1 kDa to 669.7 kDa; however, 1091 proteins (81.2%) had a MW between 20 kDa and 200 kDa. Moreover, the pI ranged from 3.78 to 12.15, with 1166 proteins (86.8%) between 4.58 and 9.38 (**Figures 4 and 5**).

GO annotation was utilized to characterize the functions of the differentially expressed proteins identified, which resulted in the classification of the proteins into three major categories: cellular component, molecular function, and biological process. As well, we characterized the top 15 annotations represented in each of the three GO categories (**Figure 6**). The cellular component category revealed that the differen-

Mitochondrial proteomic between lung adenocarcinomas and normal lung tissue

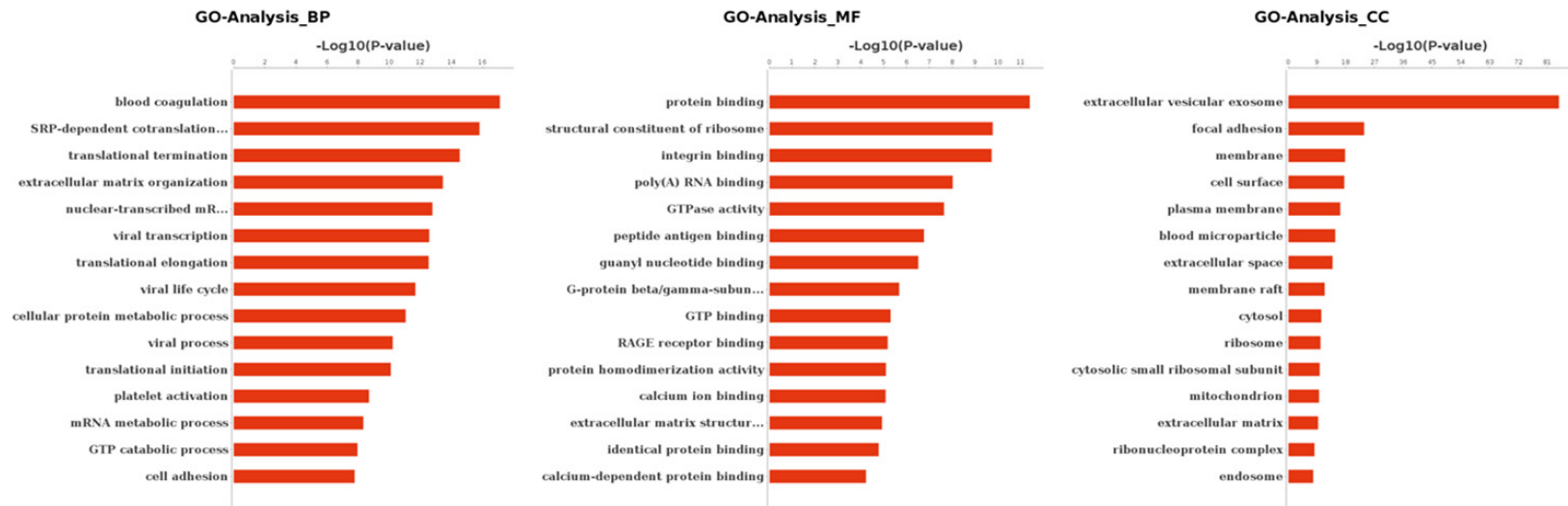


Figure 6. Significant Gene Ontology analysis of differentially expressed mitochondrial proteins (CC, Cellular component; BP, biological process; MF, molecular function).

Mitochondrial proteomic between lung adenocarcinomas and normal lung tissue

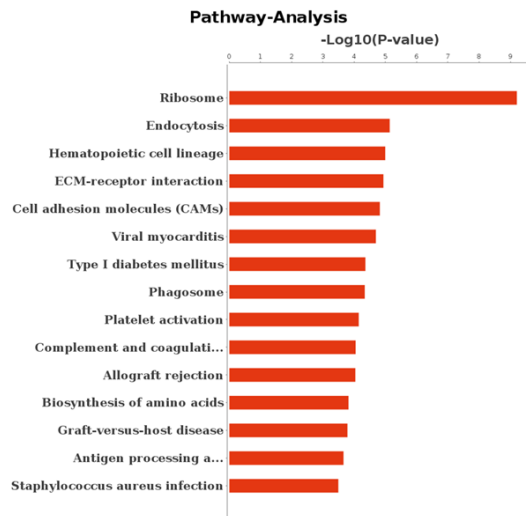


Figure 7. Significant pathway analysis of differentially expressed mitochondrial proteins.

tially expressed proteins were mainly involved in extracellular vesicular exosomes, focal adhesion, membranes, cell surface, plasma membranes, and mitochondrion. The GO annotation likewise indicated that approximately 48% of the differentially expressed proteins were mitochondrial and mitochondrial-related proteins, accounting for approximately 35.5% of the proteins detected.

In the molecular function category, the differentially expressed proteins were mainly associated with protein binding, integrin binding, poly (A) RNA binding, or functioned as structural constituents of ribosomes or in GTPase activity. The differentially expressed protein C1QBP is involved in several biological processes such as the binding of mRNA, kininogen, protein kinase C, mitochondrial ribosome, protein, complement component C1q, adrenergic receptor, hyaluronic acid, and transcription factor, or in transcription corepressor activity.

The biological process category indicated that the differentially expressed proteins were mainly related to cellular blood coagulation processes, SRP-dependent co-translational protein targeting to the membrane, translational termination, extracellular matrix organization, or nuclear-transcribed mRNA catabolic processes.

An additional pathway enrichment analysis was conducted using KEGG for the 510 differential-

ly expressed proteins. Using KEGG, we identified 63 pathways that were significantly enriched with association signals at the $p < 0.05$ level, including glycolysis/gluconeogenesis, arginine and proline metabolism, tyrosine metabolism, pyruvate metabolism, citrate cycle (TCA cycle), cell adhesion molecules (CAMs), ECM-receptor interaction, and proteoglycans in cancer. These signaling pathways are significantly affected by different proteins. And some of signaling pathways are closely related to tumors (**Figure 7**). Thus, some different proteins might be related to the occurrence and development of lung cancer.

Validation of C1QBP expression by Western blotting

To further validate the differential expression of C1QBP identified by iTRAQ labeling and LC-MS/MS, we examined C1QBP expression levels in 10 lung adenocarcinoma tissue samples and paired normal lung tissues using Western blotting. As shown in **Figure 8**, C1QBP was significantly upregulated in lung adenocarcinomas compared with matched normal lung tissues, which confirmed the LC-MS/MS results.

C1QBP expression in lung cancer and normal lung tissues

To verify the results obtained from the quantitative proteomics analysis, we performed IHC to detect the expression and cellular distribution of C1QBP in a series of 46 lung cancer specimens, including 26 adenocarcinomas and 20 lung squamous cell carcinomas, along with a series of 24 normal lung tissue specimens.

Increased expression of C1QBP was observed in the cytoplasm of the tumor cells in most of the lung adenocarcinoma specimens and in the squamous cell carcinomas (**Figure 9**). We also detected the expression of C1QBP at the nucleus of lung cancer cells, especially in phase III/IV tumors. However, negative or low C1QBP expression levels were observed in a large majority of the normal lung specimens (**Figure 9A**). Compared with normal lung specimens, the expression of C1QBP in adenocarcinomas was significantly increased ($p < 0.01$). Similarly, C1QBP expression was significantly higher in lung squamous cell carcinomas compared with normal lung tissue specimens ($p < 0.01$; **Table 2**).

Mitochondrial proteomic between lung adenocarcinomas and normal lung tissue

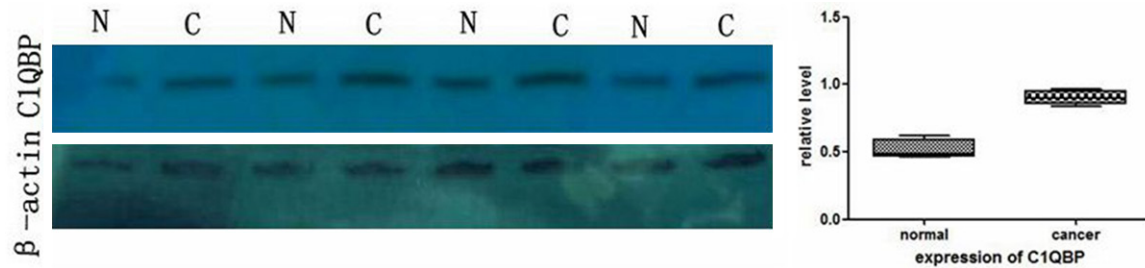


Figure 8. Expression of C1QBP in lung adenocarcinomas and paired normal lung tissues. β -actin was used as a loading control.

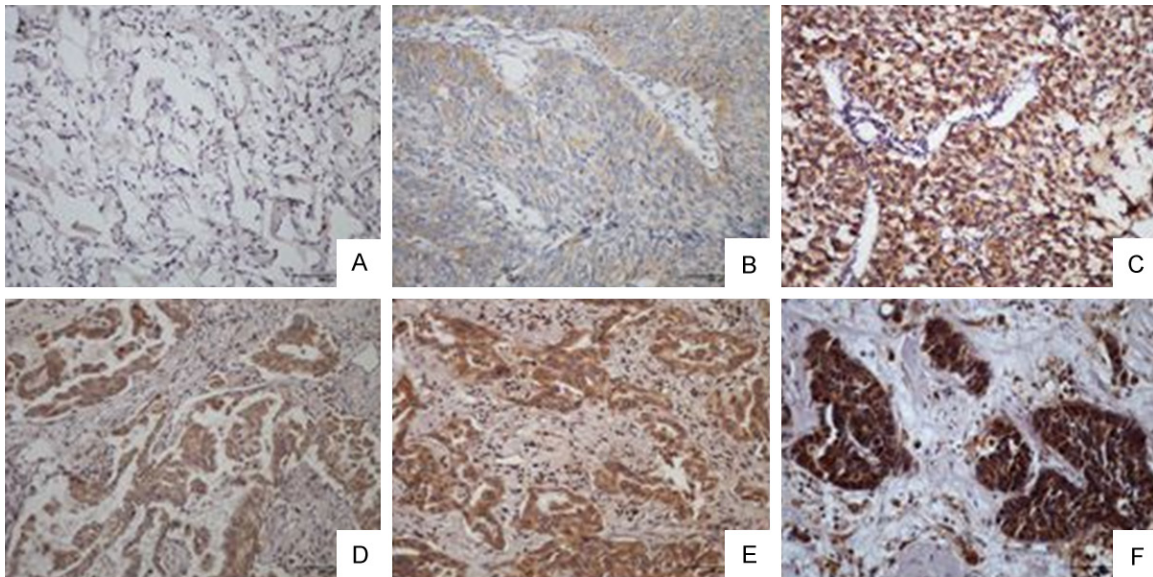


Figure 9. A. Weak staining of C1QBP in lung adenocarcinoma cell (LAC). B. Moderate staining of C1QBP in LAC. C. High staining of C1QBP in LAC. D. Negative staining in normal lung tissue. E. Weak staining of C1QBP in lung squamous cell (LSC). F. High staining of C1QBP in LSC.

Further, we summarized the relationship between clinicopathological characteristics and C1QBP expression in **Table 3**. We found that C1QBP expression is higher in stage G3 lung cancers than in stage G1/G2 tumors ($p = 0.039$). The expression of C1QBP in lung cancers with lymph node metastasis was significantly increased compared to lung cancers without lymph node metastasis ($p = 0.000$). The expression of C1QBP was likewise significantly increased in stage III/IV tumors compared with stage I/II tumors ($p = 0.000$). However, there were no significant correlations between C1QBP expression and other clinicopathological characteristics, including pathological type, patient age, gender, or tumor size (**Table 3**).

Discussion

In this study, we endeavored to detect differential protein expression between lung adenocarcinomas and normal lung tissue. Hence, our study focused on lung cancer and normal lung tissues. Because solid tumors are composed of a variety of clones or subpopulations of cancer cells, the cells within the tumor might exhibit differing properties. Thus, it is necessary to purify the target cells from the heterogeneous tissues to improve the accuracy of the results. LCM is one of the best technologies for cell purification [13]. As well, there is significant evidence suggesting that LCM can increase the specificity and sensitivity obtained from cancer tissue sections in biological and clinical-

Mitochondrial proteomic between lung adenocarcinomas and normal lung tissue

Table 2. C1QBP expression in lung cancer and normal lung tissues

Group	N	Expressional level			P-value*
		Neg	Low	High	
LAC	26	2	9	15	< 0.01 ^a
LSCC	20	1	6	13	< 0.01 ^b
LC	46	3	15	28	< 0.01 ^c
Normal	24	15	8	1	

*Mann-Whitney U test; ^aLAC versus normal lung tissue; ^bLSCC versus normal lung tissue; ^cLC versus normal lung tissue; LAC, lung adenocarcinoma; LSCC, lung squamous cell carcinoma; LC, lung cancer LCA+LSCC.

focused studies [14-17]. Hence, we obtain purified lung adenocarcinoma cells and normal lung alveolar epithelial cells using LCM.

Proteins are more diverse than DNA or RNA and contribute to the immense complexity of a biological system. Genomes and transcriptomes are relatively static and can be transcribed into a variety of functionally distinct proteins. Further, many cellular events that are mediated post-transcriptionally cannot be predicted based on the nucleic acid sequence [18]. Thus, the proteome might provide a more realistic picture of the functional aberrations that occur in cancer cells and lead to the discovery of a biomarker that could serve as a therapeutic target. Thus, we performed LCM combined with proteomics analysis to identify differentially expressed proteins in human lung adenocarcinoma and normal lung tissues, which has already been reported in prior lung cancer studies [19-21].

Mitochondria are influential in cancer initiation, growth, survival, and metastasis, and have become a research 'hot spot' in the subcellular proteomics analysis of cancer tissues. Several investigations of the tumor mitochondrial proteomes were recently conducted, including breast cancer, renal cell carcinomas, and osteosarcomas [22-24]. Purification of mitochondria or the preparation of mitochondrial-enriched protein fractions prior to proteomics analysis is critical to producing a higher yield of mitochondrial targets. Hence, we used the sucrose density gradient ultracentrifugation method in our study, which is a classical method for obtaining highly enriched mitochondrial fractions from tissues and cells, although the method is time-consuming [18]. Using this

method, we obtained purified mitochondrial proteins, which we confirmed by Western blotting.

Our study combined the use of LCM with proteomics, and obtained purified mitochondrial proteins. Quantitative proteomics techniques have recently emerged as a robust tool for uncovering differential protein expression associated with the mechanisms and therapeutic targets of natural products. Several prior studies have focused on lung cancer [25, 26]. As well, several alternative technologies for the separation, identification, and quantification of alterations in the proteome are available, each with particular strengths and limitations. Traditional two-dimensional gel electrophoresis (2-DE) techniques have been widely used in comparative proteomics and are associated with significant advances, but 2-DE has several disadvantages. 2-DE is less than satisfactory when extensive sample handling is required. As well, 2-DE is also less accurate for the identification of low abundance proteins, proteins with high MW and *pI* values, and for hydrophobic proteins [27, 28]. At present, iTRAQ is the most widely used method for high-throughput protein quantitation, as it allows the simultaneous quantification of multiple biological samples [29, 30]. As well, this technology has been successfully used to identify differentially expressed proteins in lung adenocarcinoma cell lines [31]. Bottom-up proteomics approaches that combine LC for peptide separation with tandem MS for identification and quantification (LC-MS/MS) are becoming increasingly popular due to improvements in instrumentation and quantification approaches [30]. Likewise, recent advances have made it possible to seek novel molecular markers using large-scale proteomics for the diagnosis, outcome prediction, and identification of molecules involved in carcinogenesis during tumor development.

In the present study, we utilized comparative proteomics to identify differentially expressed proteins in lung cancer and normal tissues, and found that the expression of C1QBP was significantly different between lung cancer and normal tissues. C1QBP (Complement component 1 Q subcomponent-binding protein, also p32/gC1qR/HABP1) is a highly anionic, 33 kDa cellular protein that was initially identified and characterized as the gC1q receptor for comple-

Mitochondrial proteomic between lung adenocarcinomas and normal lung tissue

Table 3. Association between C1QBP expression and clinicopathological characteristics of lung cancers

Characteristics	No.	C1QBP expression			P-value
		Negative	Low	High	
Gender					
Male	30	1	9	20	0.531
Female	16	2	6	8	
Age					
< 60	25	1	9	15	0.489
≥ 60	21	2	6	13	
Grade					
G1/G2	23	1	11	11	0.039
G3	23	2	4	17	
Histology type					
LC	26	2	9	15	0.990
LSCC	20	1	6	13	
TNM stage					
I/II	25	1	10	14	0.000
III/IV	21	2	5	14	
Lymphatic invasion					
N0	24	1	10	13	0.000
N+	22	2	5	15	
Tumor size					
< 3	17	1	6	10	0.810
3 ≤ T < 7	25	2	8	15	
≥ 7	4	0	1	3	

P-values by Mann-Whitney U test or Kruskal-Wallis test.

ment component C1q [32]. C1QBP was also thought to be a link to autophagy [33], a key molecule in oxidative phosphorylation [34], a regulator of tumor metabolism, and a mediator of cellular apoptosis [35] in mitochondria; thus, it might be involved in cancer progression.

In our study, we detected the differential expression of C1QBP in mitochondria between lung cancer and normal tissues by Western blotting. Other studies have also indicated that C1QBP is localized in the mitochondria but not in the nucleus in prostate cancer cell lines [36-38]. However, it was also reported that C1QBP is localized predominantly in the mitochondrial matrix but is also present at the cell surface [39] and in the nucleus [40-42]. RieAmamoto found that the nuclear expression of p32 was significantly increased in prostate cancer with a higher Gleason score, pathological stage, and preoperative prostate-specific antigen level, suggesting that the nuclear function of p32

might be involved in tumor progression. We found obvious differences in C1QBP expression in the mitochondria of lung adenocarcinoma cells versus normal alveolar epithelial cells. In our immunohistochemistry analyses, we detected the expression of C1QBP in the mitochondria and in the nucleus in the tissues analyzed, especially in tissues with high C1QBP staining (**Figure 9C-F**), which suggests the differential localization of C1QBP in different cell types under different physiological conditions, including cancer. Further, the nuclear expression of C1QBP might be associated with an interaction with nuclear proteins such as alternate mRNA splicing factor SF2 [40] and LaminB receptor [43].

The current study is the first to demonstrate the relationship between clinicopathological factors and the expression of p32 in patients with lung cancer. The overexpression of C1QBP has been described in human adenocarcinomas of the breast [44], thyroid, colon, pancreas, stomach, esophagus, and lung relative to corresponding nonmalignant tissues [45]. Likewise, immunohistochemistry results have revealed that HABP1 expression in breast cancer cells is higher than levels detected in normal breast cells. A multivariate analysis revealed that the expression of C1QBP was a significant factor for predicting prognosis and indicated that the expression of C1QBP in prostate tumor samples was significantly associated with the Gleason score, pathological stage, and relapse. These data suggested that C1QBP is critical for the proliferation of prostate cancer cells and might be a novel marker of clinical progression in prostate cancer. In our study, C1QBP was highly expressed in lung cancer samples and its expression was significantly associated with the pathological grade, TNM stage, and lymph node metastasis. These data suggest that C1QBP is also critical for lung cancer and might be a novel marker of clinical progression in lung cancer.

However, Ghosh et al [46] reported the detection of C1QBP expression in normal proliferating cells, benign inflammatory lesions, and epithelial-derived malignancies [47]. In particular, the absence of C1QBP might have a strong negative predictive value for ruling out a pathologic process involving epithelial cells. Thus, for C1QBP to be considered a biomarker, further

studies on the expression of C1QBP in other lung diseases, such as pneumonia and tuberculosis, are required.

In conclusion, we used iTRAQ-labeling combined with 2D LC-MS/MS and identified 510 differentially expressed mitochondrial proteins in lung adenocarcinoma and normal lung tissue. We likewise selectively verified the expression of the mitochondrial protein C1QBP, which exhibited differential expression in the cancerous and normal lung tissues. The current study is the first to demonstrate the relationship between clinicopathological factors and the expression of C1QBP in patients with lung cancer. To be verified as a biomarker of lung cancer, additional studies of the expression of C1QBP in other benign lung diseases are required. Nonetheless, our findings could have potential clinical value in the diagnosis of lung cancer, and provide valuable information for future studies of the molecular mechanisms of mitochondria during lung cancer.

Acknowledgement

This study was funded by the National Natural Science Foundation of China (Grant No. 81172234) and the Natural Science Basic research Foundation of Shaanxi Province, China. (Grant No. 2014JM2-8162).

Disclosure of conflict of interest

None.

Address correspondence to: Dr. Shuanying Yang, Department of Respiratory Medicine, Second Affiliated Hospital of Xi'an Jiaotong University, NO. 157 Xiwu Road, Xi'an 710004, Shaanxi Province, P. R. China. Fax: +86-02987678599; E-mail: yangshuanying66@163.com

References

- [1] Siegel RL, Miller KD and Jemal A. Cancer statistics, 2017. *CA Cancer J Clin* 2017; 67: 7-30.
- [2] Chen W, Zheng R, Baade PD, Zhang S, Zeng H, Bray F, Jemal A, Yu XQ and He J. Cancer statistics in China, 2015. *CA Cancer J Clin* 2016; 66: 115-132.
- [3] Jemal A, Bray F, Center MM, Ferlay J, Ward E and Forman D. Global cancer statistics. *CA Cancer J Clin* 2011; 61: 69-90.
- [4] Siegel RL, Miller KD and Jemal A. Cancer statistics, 2015. *CA Cancer J Clin* 2015; 65: 5-29.
- [5] Graves JA, Wang Y, Sims-Lucas S, Cherek E, Rothermund K, Branca MF, Elster J, Beer-Stolz D, Van Houten B, Vockley J and Prochownik EV. Mitochondrial structure, function and dynamics are temporally controlled by c-Myc. *PLoS One* 2012; 7: e37699.
- [6] Sarosiek KA, Chi X, Bachman JA, Sims JJ, Montero J, Patel L, Flanagan A, Andrews DW, Sorger P and Letai A. BID preferentially activates BAK while BIM preferentially activates BAX, affecting chemotherapy response. *Mol Cell* 2013; 51: 751-765.
- [7] Berkers CR, Maddocks OD, Cheung EC, Mor I and Vousden KH. Metabolic regulation by p53 family members. *Cell Metab* 2013; 18: 617-633.
- [8] Verma M, Kagan J, Sidransky D and Srivastava S. Proteomic analysis of cancer-cell mitochondria. *Nat Rev Cancer* 2003; 3: 789-795.
- [9] Vyas S, Zaganjor E and Haigis MC. Mitochondria and Cancer. *Cell* 2016; 166: 555-566.
- [10] Suarez-Quian CA, Goldstein SR, Pohida T, Smith PD, Peterson JI, Wellner E, Ghany M and Bonner RF. Laser capture microdissection of single cells from complex tissues. *Biotechniques* 1999; 26: 328-335.
- [11] Ashburner M, Ball CA, Blake JA, Botstein D, Butler H, Cherry JM, Davis AP, Dolinski K, Dwight SS, Eppig JT, Harris MA, Hill DP, Issel-Tarver L, Kasarskis A, Lewis S, Matese JC, Richardson JE, Ringwald M, Rubin GM and Sherlock G. Gene ontology: tool for the unification of biology. The gene ontology consortium. *Nat Genet* 2000; 25: 25-29.
- [12] Yu H, Liu Q, Xin T, Xing L, Dong G, Jiang Q, Lv Y, Song X, Teng C, Huang D, Li Y, Shen W, Teng C, Jin Y and Zhang F. Elevated expression of hyaluronic acid binding protein 1 (HABP1)/P32/C1QBP is a novel indicator for lymph node and peritoneal metastasis of epithelial ovarian cancer patients. *Tumour Biol* 2013; 34: 3981-3987.
- [13] Emmert-Buck MR, Bonner RF, Smith PD, Chuaqui RF, Zhuang Z, Goldstein SR, Weiss RA and Liotta LA. Laser capture microdissection. *Science* 1996; 274: 998-1001.
- [14] Chowdhuri SR, Xi L, Pham TH, Hanson J, Rodriguez-Canales J, Berman A, Rajan A, Giaccone G, Emmert-Buck M, Raffeld M and Filie AC. EGFR and KRAS mutation analysis in cytologic samples of lung adenocarcinoma enabled by laser capture microdissection. *Mod Pathol* 2012; 25: 548-555.
- [15] El-Serag HB, Nurgalieva ZZ, Mistretta TA, Finegold MJ, Souza R, Hilsenbeck S, Shaw C and Darlington G. Gene expression in Barrett's esophagus: laser capture versus whole tissue. *Scand J Gastroenterol* 2009; 44: 787-795.

Mitochondrial proteomic between lung adenocarcinomas and normal lung tissue

- [16] Harrell JC, Dye WW, Harvell DM, Sartorius CA and Horwitz KB. Contaminating cells alter gene signatures in whole organ versus laser capture microdissected tumors: a comparison of experimental breast cancers and their lymph node metastases. *Clin Exp Metastasis* 2008; 25: 81-88.
- [17] Klee EW, Erdogan S, Tillmans L, Kosari F, Sun Z, Wigle DA, Yang P, Aubry MC and Vasmatzis G. Impact of sample acquisition and linear amplification on gene expression profiling of lung adenocarcinoma: laser capture micro-dissection cell-sampling versus bulk tissue-sampling. *BMC Med Genomics* 2009; 2: 13.
- [18] Taylor SW, Fahy E, Zhang B, Glenn GM, Warnock DE, Wiley S, Murphy AN, Gaucher SP, Capaldi RA, Gibson BW and Ghosh SS. Characterization of the human heart mitochondrial proteome. *Nat Biotechnol* 2003; 21: 281-286.
- [19] Bu LN, Yang SY, Li FT, Shang WL, Zhang W, Huo SF, Nan YD, Tian YX, Du J, Lin XL, Liu YF, Lin YR and Rong BX. Study of differential proteins in lung adenocarcinoma using laser capture microdissection combined with liquid chip-mass spectrometry technology. *Chin Med J (Engl)* 2010; 123: 3309-3313.
- [20] Zhang X, Li W, Hou Y, Niu Z, Zhong Y, Zhang Y and Yang S. Comparative membrane proteomic analysis between lung adenocarcinoma and normal tissue by iTRAQ labeling mass spectrometry. *Am J Transl Res* 2014; 6: 267-280.
- [21] Xu Y, Cao LQ, Jin LY, Chen ZC, Zeng GQ, Tang CE, Li GQ, Duan CJ, Peng F, Xiao ZQ and Li C. Quantitative proteomic study of human lung squamous carcinoma and normal bronchial epithelial acquired by laser capture microdissection. *J Biomed Biotechnol* 2012; 2012: 510418.
- [22] Strong R, Nakanishi T, Ross D and Fenselau C. Alterations in the mitochondrial proteome of adriamycin resistant MCF-7 breast cancer cells. *J Proteome Res* 2006; 5: 2389-2395.
- [23] Craven RA, Hanrahan S, Totty N, Harnden P, Stanley AJ, Maher ER, Harris AL, Trimble WS, Selby PJ and Banks RE. Proteomic identification of a role for the von Hippel Lindau tumour suppressor in changes in the expression of mitochondrial proteins and septin 2 in renal cell carcinoma. *Proteomics* 2006; 6: 3880-3893.
- [24] Chevallet M, Lescuyer P, Diemer H, van Dorselaer A, Leize-Wagner E and Rabilloud T. Alterations of the mitochondrial proteome caused by the absence of mitochondrial DNA: a proteomic view. *Electrophoresis* 2006; 27: 1574-1583.
- [25] Deng W, Yan M, Yu T, Ge H, Lin H, Li J, Liu Y, Geng Q, Zhu M, Liu L, He X and Yao M. Quantitative proteomic analysis of the metastasis-inhibitory mechanism of miR-193a-3p in non-small cell lung cancer. *Cell Physiol Biochem* 2015; 35: 1677-1688.
- [26] Walker MJ, Zhou C, Backen A, Pernemalm M, Williamson AJ, Priest LJ, Koh P, Faivre-Finn C, Blackhall FH, Dive C and Whetton AD. Discovery and validation of predictive biomarkers of survival for non-small cell lung cancer patients undergoing radical radiotherapy: two proteins with predictive value. *E Bio Medicine* 2015; 2: 841-850.
- [27] Gilmore JM and Washburn MP. Advances in shotgun proteomics and the analysis of membrane proteomes. *J Proteomics* 2010; 73: 2078-2091.
- [28] Elamin A, Titz B, Dijon S, Merg C, Geertz M, Schneider T, Martin F, Schlage WK, Frentzel S, Talamo F, Phillips B, Veljkovic E, Ivanov NV, Vanscheeuwijck P, Peitsch MC and Hoeng J. Quantitative proteomics analysis using 2D-PAGE to investigate the effects of cigarette smoke and aerosol of a prototypic modified risk tobacco product on the lung proteome in C57BL/6 mice. *J Proteomics* 2016; 145: 237-245.
- [29] Feng H, Li X, Niu D and Chen WN. Protein profile in HBx transfected cells: a comparative iTRAQ-coupled 2D LC-MS/MS analysis. *J Proteomics* 2010; 73: 1421-1432.
- [30] Zieske LR. A perspective on the use of iTRAQ reagent technology for protein complex and profiling studies. *J Exp Bot* 2006; 57: 1501-1508.
- [31] Cui YQ, Geng Q, Yu T, Zhang FL, Lin HC, Li J, Zhu MX, Liu L, Yao M and Yan MX. Establishment of a highly metastatic model with a newly isolated lung adenocarcinoma cell line. *Int J Oncol* 2015; 47: 927-940.
- [32] Ghebrehiwet B, Silvestri L and McDevitt C. Identification of the Raji cell membrane-derived C1q inhibitor as a receptor for human C1q. Purification and immunochemical characterization. *J Exp Med* 1984; 160: 1375-1389.
- [33] Reef S, Shifman O, Oren M and Kimchi A. The autophagic inducer smARF interacts with and is stabilized by the mitochondrial p32 protein. *Oncogene* 2007; 26: 6677-6683.
- [34] Sengupta A, Banerjee B, Tyagi RK and Datta K. Golgi localization and dynamics of hyaluronan binding protein 1 (HABP1/p32/C1QBP) during the cell cycle. *Cell Res* 2005; 15: 183-186.
- [35] Kamal A and Datta K. Upregulation of hyaluronan binding protein 1 (HABP1/p32/gC1qR) is associated with Cisplatin induced apoptosis. *Apoptosis* 2006; 11: 861-874.
- [36] Amamoto R, Yagi M, Song Y, Oda Y, Tsuneyoshi M, Naito S, Yokomizo A, Kuroiwa K, Tokunaga S, Kato S, Hiura H, Samori T, Kang D and Uchi-

Mitochondrial proteomic between lung adenocarcinomas and normal lung tissue

- umi T. Mitochondrial p32/C1QBP is highly expressed in prostate cancer and is associated with shorter prostate-specific antigen relapse time after radical prostatectomy. *Cancer Sci* 2011; 102: 639-647.
- [37] Muta T, Kang D, Kitajima S, Fujiwara T and Hamasaki N. p32 protein, a splicing factor 2-associated protein, is localized in mitochondrial matrix and is functionally important in maintaining oxidative phosphorylation. *J Biol Chem* 1997; 272: 24363-24370.
- [38] Soltys BJ, Kang D and Gupta RS. Localization of P32 protein (gC1q-R) in mitochondria and at specific extramitochondrial locations in normal tissues. *Histochem Cell Biol* 2000; 114: 245-255.
- [39] Ghebrehiwet B, Lim BL, Peerschke EI, Willis AC and Reid KB. Isolation, cDNA cloning, and over-expression of a 33-kD cell surface glycoprotein that binds to the globular "heads" of C1q. *J Exp Med* 1994; 179: 1809-1821.
- [40] Matthews DA and Russell WC. Adenovirus core protein V interacts with p32—a protein which is associated with both the mitochondria and the nucleus. *J Gen Virol* 1998; 79: 1677-1685.
- [41] Majumdar M, Meenakshi J, Goswami SK and Datta K. Hyaluronan binding protein 1 (HABP1)/C1QBP/p32 is an endogenous substrate for MAP kinase and is translocated to the nucleus upon mitogenic stimulation. *Biochem Biophys Res Commun* 2002; 291: 829-837.
- [42] Brokstad KA, Kalland KH, Russell WC and Matthews DA. Mitochondrial protein p32 can accumulate in the nucleus. *Biochem Biophys Res Commun* 2001; 281: 1161-1169.
- [43] Marschall M, Marzi A, aus dem Siepen P, Jochmann R, Kalmer M, Auerochs S, Lischka P, Leis M and Stamminger T. Cellular p32 recruits cytomegalovirus kinase pUL97 to redistribute the nuclear lamina. *J Biol Chem* 2005; 280: 33357-33367.
- [44] Chen YB, Jiang CT, Zhang GQ, Wang JS and Pang D. Increased expression of hyaluronic acid binding protein 1 is correlated with poor prognosis in patients with breast cancer. *J Surg Oncol* 2009; 100: 382-386.
- [45] Rubinstein DB, Stortchevoi A, Boosalis M, Ashfaq R, Ghebrehiwet B, Peerschke EI, Calvo F and Guillaume T. Receptor for the globular heads of C1q (gC1q-R, p33, hyaluronan-binding protein) is preferentially expressed by adenocarcinoma cells. *Int J Cancer* 2004; 110: 741-750.
- [46] Ghosh I, Chowdhury AR, Rajeswari MR and Datta K. Differential expression of Hyaluronic Acid Binding Protein 1 (HABP1)/P32/C1QBP during progression of epidermal carcinoma. *Mol Cell Biochem* 2004; 267: 133-139.
- [47] Dembitzer FR, Kinoshita Y, Burstein D, Phelps RG, Beasley MB, Garcia R, Harpaz N, Jaffer S, Thung SN, Unger PD, Ghebrehiwet B and Peerschke EI. gC1qR expression in normal and pathologic human tissues: differential expression in tissues of epithelial and mesenchymal origin. *J Histochem Cytochem* 2012; 60: 467-474.